

# Development of a mathematical equation describing the strain hardening behaviour of metastable AISI 301 austenitic stainless steel

T W Mukarati<sup>1,\*</sup>, R J Mostert<sup>1</sup> and C W Siyasiya<sup>1</sup>

<sup>1</sup> University of Pretoria, Private bag X20 Hatfield 0028, South Africa

\*E-mail: Corresponding Author: [tmcarati@gmail.com](mailto:tmcarati@gmail.com)

**Abstract.** The strain hardening behaviour of AISI 301 metastable austenite steel was analysed by evaluating tensile data against the empirical mathematical equations of Hollomon, Ludwik and Ludwison. It was found that these equations were inadequate to model this TRIP steel with low stacking fault energy (SFE). It was found that the fraction of strain-induced martensite could be expressed as a sigmoidal function of the applied strain. The log-log plots of true stress and true plastic strain from 5% to  $\epsilon_{UTS}$  performed with uniaxial isothermal tests at 30 °C were thereafter adequately fitted with a sigmoidal curve. The instantaneous strain hardening exponent was determined as the slope of the above-mentioned sigmoidal curve at a specific strain value. The strain hardening exponent and the rate of strain hardening ( $d\sigma/d\epsilon$ ) increases with deformation due to formation of strain-induced martensite to a maximum and thereafter decreases as the volume fraction of strain-induced martensite approximates saturation. The variation of the instantaneous strain hardening exponent as a function of plastic strain and the strength coefficient, K, at 30 °C was deduced. A high value of K, 1526MPa, was determined. A correlation between the extent of martensitic transformation and the value of the instantaneous strain hardening exponent was observed. This work is part of the project that seeks to develop a constitutive model describing the flow stress during plastic deformation as a function of both plastic strain and the resulting martensitic transformation at different temperatures and strain rates and which accounts for the isotropic hardening process.

## 1. Introduction

The work-hardening behaviour of many engineering materials have been sufficiently described by the Hollomon power law [1]:

$$\sigma = K\epsilon^n \quad (1)$$

where  $\sigma$  is the true stress; K is the strength coefficient,  $\epsilon$  is true plastic strain and n is the strain hardening exponent. The Ludwik model has an additional stress factor ( $\sigma_0$ ) for materials which show a varied yield strength with similar strain hardening [1].

$$\sigma = \sigma_0 + K\epsilon^n \quad (2)$$

An equation with an additional strain term,  $\epsilon_0$ , which accounts for pre-strain was proposed by Swift, for materials which show similar yield strength with varied strain hardening behaviour [1].

$$\sigma = K (\epsilon_0 + \epsilon)^n \quad (3)$$



For stable austenitic stainless steels, although the Hollomon or Ludwik equations can describe the plastic flow behaviour at high strain levels, the models were found to be insufficient in describing the plastic flow behaviour and work hardening at low strain values [2]. A modified Ludwik model was then proposed by Ludwigson to consider the deviation [3].

$$\sigma = K\varepsilon^n + \Delta \quad (4)$$

where the deviation  $\Delta = \exp(K_1)\exp(n_1\varepsilon)$ .  $K$  and  $n$  have the same meaning as in the Hollomon equation and  $\exp(K_1) \approx$  proportional limit and  $n_1$  is the slope of the deviation of stress from the Hollomon equation plotted against true strain,  $\varepsilon$  [3].

The Voce flow stress relationship for materials which show saturation stress at high stress/strain levels can be represented as follows [1]:

$$\sigma = \sigma_s - (\sigma_s - \sigma_1)\exp[-(\varepsilon - \varepsilon_1)/\varepsilon_c] \quad (5)$$

where  $\sigma_s$ , is the saturation stress,  $\sigma_1$  and  $\varepsilon_1$  are the true stress and true plastic strain values at the onset of plastic deformation, respectively, and  $\varepsilon_c$  is a constant. The Voce stress relationship is usually applicable only at high temperatures where dynamic recovery cancel out the work hardening effect during the test.

In the current work, the strain hardening behaviour of a metastable AISI 301 steel (for chemical composition see reference [4]) was investigated with a view to establish a single mathematical equation that describes the behaviour adequately.

The Ludwikson modification has earlier been found to be adequate in describing the tensile flow and work hardening behaviour of ferritic stainless steels [1]. There was no information which was found in literature about applicability of the Ludwikson equation in describing the work hardening behaviour of metastable austenitic stainless steels which undergo a phase transformation during deformation.

## 2. Experimental procedure

The plastic flow behaviour was studied by means of uniaxial tensile testing. Interrupted uniaxial tensile test was done at 30 °C using an Instron-type tensile machine (1175 model) fitted with an environmental chamber (3110 model) at a strain rate of  $6.67 \times 10^{-4}\text{s}^{-1}$ . A 50 mm gauge length extensometer (Instron-type model 2630-112) was used to determine the elongation of the samples. An indication of the percentage of  $\alpha'$ -martensite of all the specimens was initially determined using a Ferritescope (Helmut Fisher GmbH, model MP3B) at 5% engineering strain intervals. The device was calibrated using standard  $\delta$ -ferrite samples supplied with it. Seven readings were taken on each sample at different points within the gauge length on the surface.

A calibration curve was later developed using X-ray diffraction to determine the percentage of  $\alpha'$ -martensite from the Ferritescope measurements [5]:

$$\text{True } \alpha'\text{-martensite content} = 1.81 \times \text{Ferritescope reading} \quad (6)$$

## 3. Results

Figures 1 (a) and (b) show the engineering stress-strain curve and the true stress-true strain curves at a temperature of 30 °C, respectively. Figure 1(b) excludes tensile data points beyond the necking onset. Figure 2 shows the plastic flow log-log plot of true stress and true strain at temperature of 30 °C. Figures 3 (a) and (b) show a sigmoidal fit applied to the experimental data points of the fraction of martensite as a function of strain at 30 °C. The fraction of martensite transformed strain sensitivity obtained by differentiation of the curve in Figure 3 (a) is shown in Figure 3 (b).

Figures 4 (a) and (b) show the log-log plot of true stress-strain at temperature of 30 °C for a true strain of (a) less than 5% which shows that Hollomon fit has only been obeyed at low plastic strain with a strain hardening exponent,  $n$  of 0.11 and (b) at strains greater than 5% showing a sigmoidal flow stress relationship. Figure 5 (a) shows the variation of instantaneous strain hardening exponent as a function of increasing plastic strain for true strain values above 5%, given by the slope of Fig 4(b) utilising a

number of tangent lines as a function of true strain. Figure 5(b) is a superimposition of Figure 3(a) and 4 (b) showing a correlation of the tensile flow stress and percentage of martensite transformed curves. Figure 6 (a) is a superimposition of Figure 3(b) and 5(a) showing peak instantaneous  $\alpha'$ -martensite transformation strain sensitivity,  $(dV\alpha'/(d\epsilon)^{-1})$  and peak instantaneous strain hardening exponent ( $n_i$ ) as a function of strain. Figure 6 (b) shows the strength (log true stress) as a function of the percentage of martensite formed.

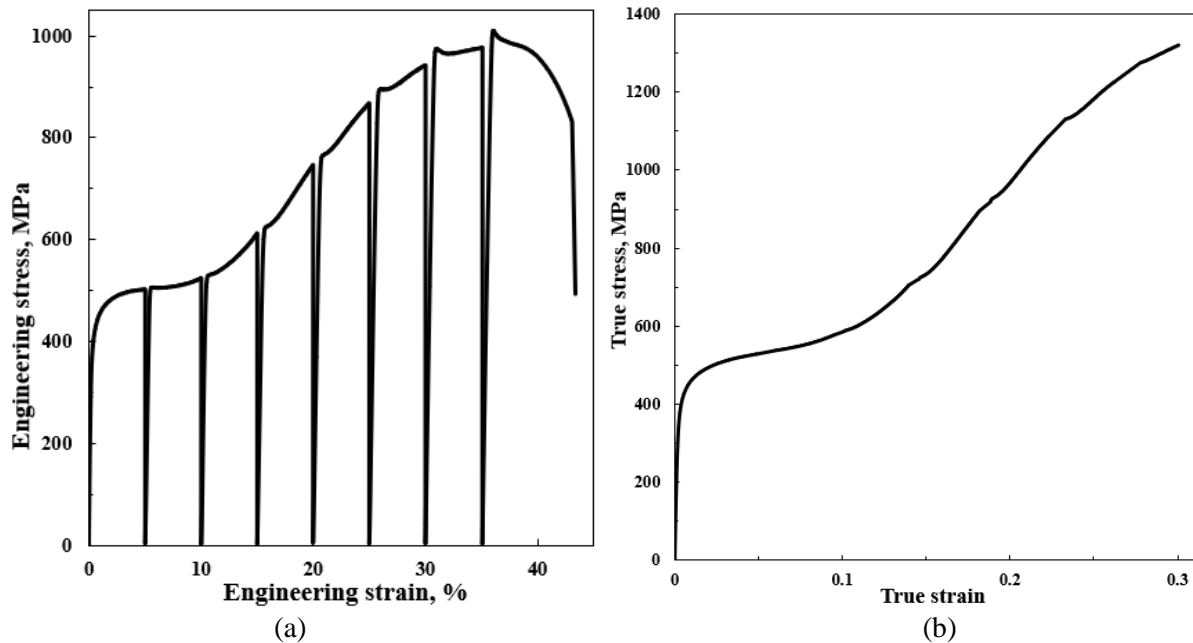


**Figure 1:** (a) Interrupted engineering stress-strain curve (b) True stress-true strain curve at a temperature of 30 °C.

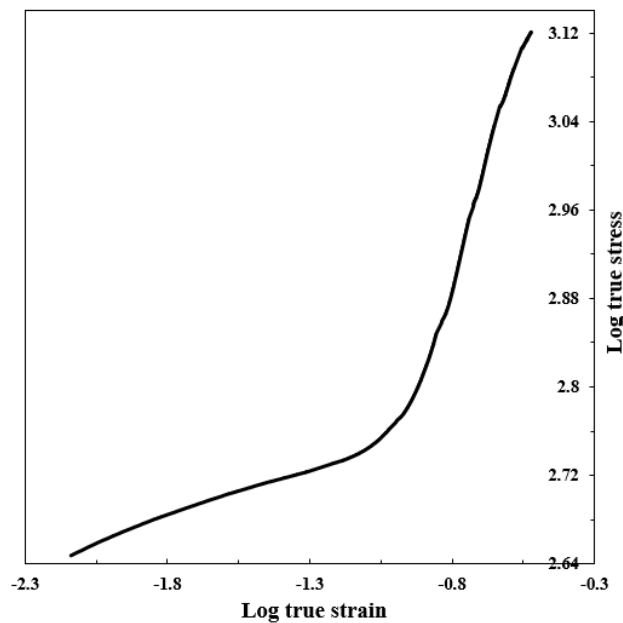


**Figure 2:** The plastic flow log-log plot of true stress and true strain at temperature of 30 °C from  $R_p$  to  $R_m$

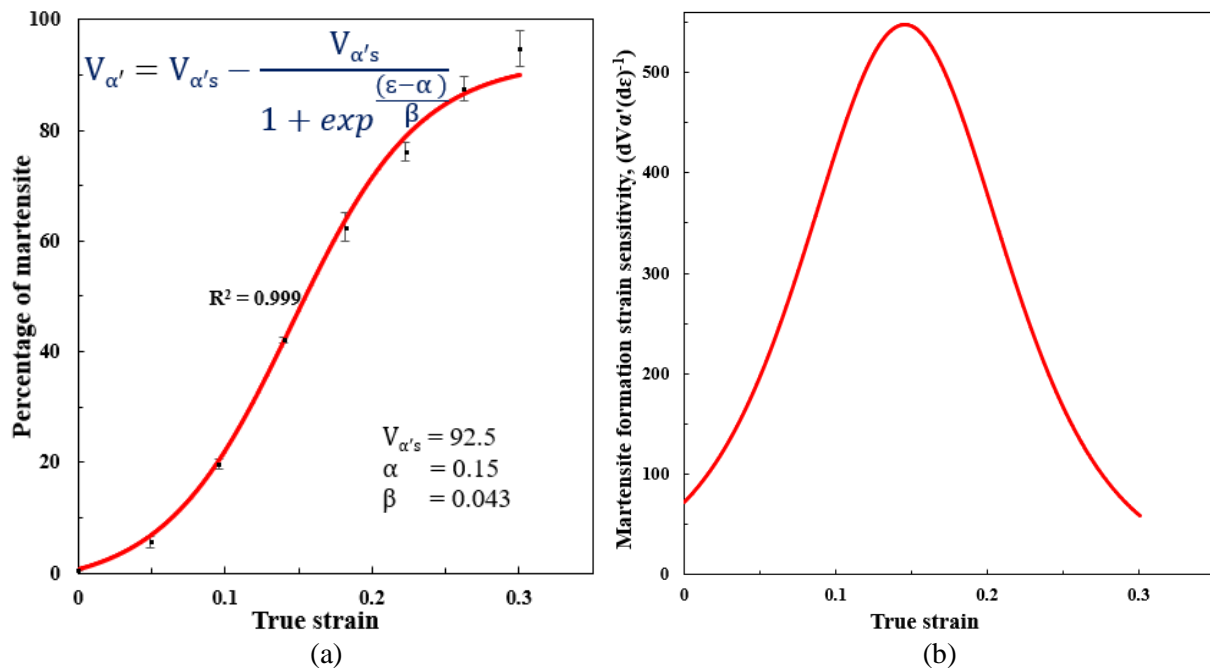


**Figure 3:** (a) Percentage of  $\alpha'$ -martensite as a function of strain at 30 °C (fitted sigmoidal curve) (b)  $\alpha'$ -martensite transformation strain sensitivity,  $(dV_{\alpha'}(d\epsilon)^{-1})$  (dimensionless) obtained by differentiation of the curve in Figure 3 (a).

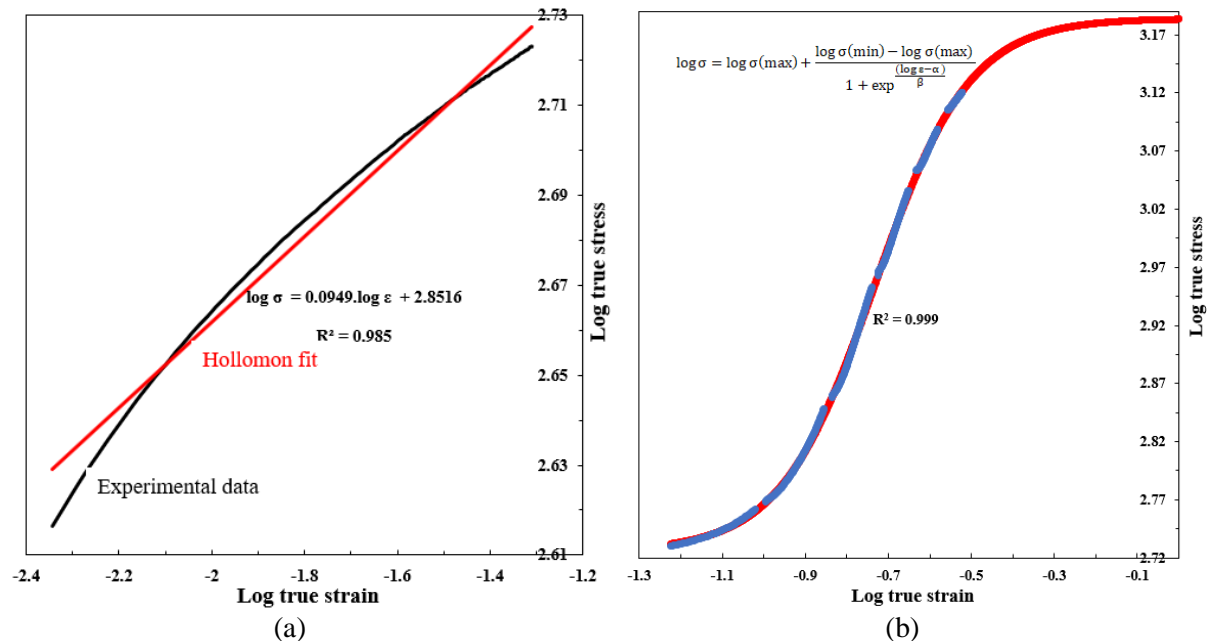


**Figure 4:** The log-log plot of true stress-strain at a temperature of 30 °C for true strain of (a) less than 5% (obeying the Hollomon equation) and (b) greater than 5%, showing sigmoidal flow stress behaviour (sigmoidal equation given in the figure with constants given in equation 7). [The blue line in both Figure 4 (a) and (b) represents the experimental log-log plot of true stress-strain curve whilst the red line is a Hollomon fit in Figure 4 (a) and a sigmoidal fit in Figure 4 (b) which was extrapolated to a log true strain value of 0 to determine the strength coefficient, K.]

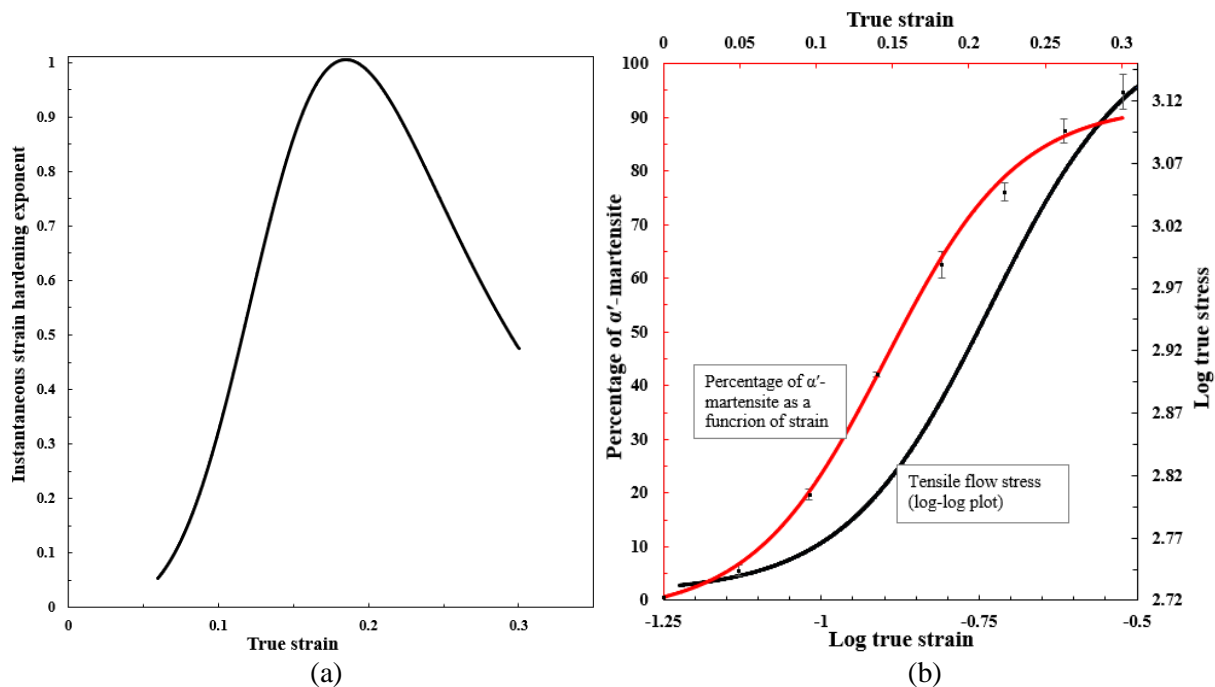


**Figure 5:** (a) Variation of instantaneous strain hardening exponent,  $n_i$  with deformation for true strain above 5% (b) Superimposition of Figure 3(a) and 4 (b) showing a correlation of tensile flow stress with percentage of martensite transformed.

The instantaneous strain hardening exponent, (refer to Soares et al) [6] was found to generally increase with deformation due to the strain-induced martensitic transformation (SIMT). After an initial linear portion (up to  $\epsilon = 0.05$ ), the strain hardening behaviour becomes non-linear (Fig 4(b)), with strong strain hardening experienced, due to SIMT as shown in Figure 5(a) and 5(b).

The instantaneous strain hardening exponent was found to be variable with a peak value of 1.00 at a strain value of 0.19 and  $\log K$  was found to be 3.18. The coefficient of strength,  $K$  is therefore approximately 1526 MPa as determined by an extrapolation of the sigmoidal curve to a true strain value of 1. The high value of strength is attributed to the high percentage of transformed martensite, above 90% as shown in Figure 3 (a).

It is apparent from Figure 6 (a) that the curve describing the martensite formation strain sensitivity as a function of strain has a similar shape to the instantaneous strain hardening exponent curve. However, the peak instantaneous derivative of  $\alpha'$ -martensitic transformation was reached at lower strain than the peak instantaneous strain hardening exponent. This depicts that the strain hardening behaviour of AISI 301 steel is controlled by the formation of strain-induced  $\alpha'$ -martensite [7]. The strength of the material is directly proportional to the percentage of martensite evolved during deformation as shown in Figure 6 (b).

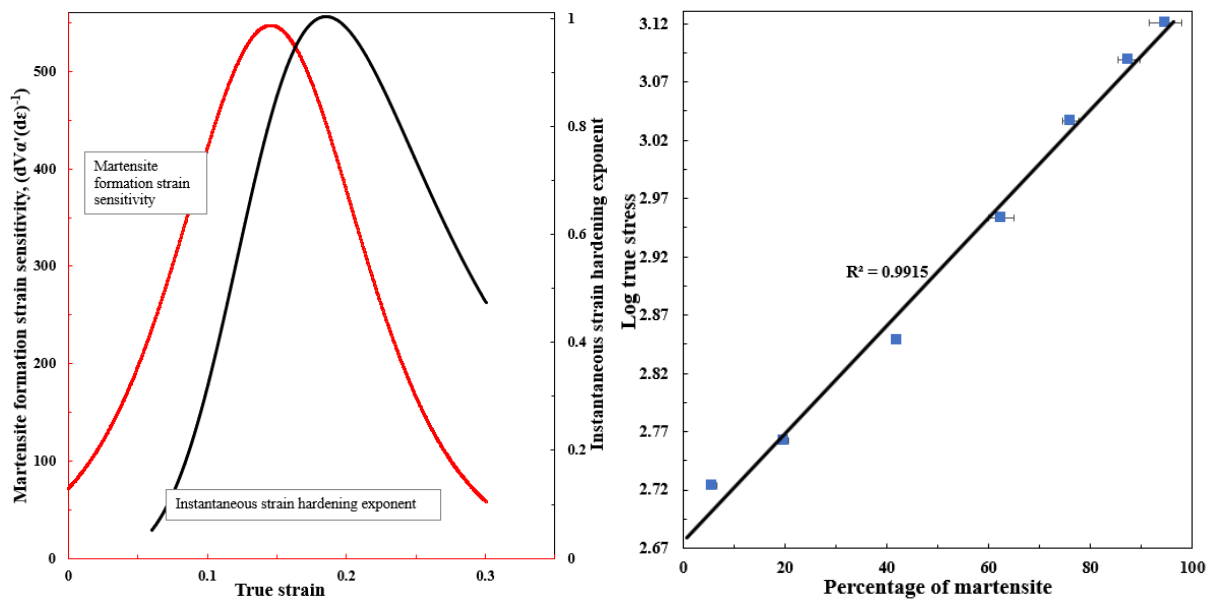


**Figure 6:** (a) Superimposition of Figure 3(b) and 5(a) showing peak instantaneous  $\alpha'$ -martensite transformation strain sensitivity,  $(dV\alpha'(d\epsilon)^{-1})$  and peak instantaneous strain hardening exponent,  $n_i$  as a function of strain (b) the strength as a function of percentage of martensite.

#### 4. Discussion

The AISI 301 alloy tested here is a lean alloyed stainless steel with high nitrogen content and very low stacking fault energy at room temperature which makes it amenable to SIMT leading to a strong increase in strain hardening with increased applied strain.

Due to the flow behaviour associated with strain-induced martensitic transformation, a sigmoidal equation was found to be the only mathematical relationship adequately describing the strain hardening of this steel, above plastic true strain levels of 0.05.

The mathematical sigmoidal function established in the true strain range from 0.05 to  $\epsilon_u$  (strain corresponding to maximum load) is given by:

$$\log \sigma = A + (B - A)[1 + \exp(\log \epsilon - \alpha)(\beta)^{-1}]^{-1} \quad [7]$$

with  $R^2 = 0.999$ , at 30 °C.

Where,

$\sigma$  is the true stress in MPa,

A is the maximum log of true stress ( $\log \sigma_{\max}$ ) when the sigmoidal function levels off after the martensitic transformation reaches saturation point (value of 3.18 at 30 °C and strain rate of  $6.67 \times 10^{-4} \text{ s}^{-1}$ ).

B is the minimum log of true stress ( $\log \sigma_{\min}$ ) before any martensitic transformation (value of 2.73 at 30 °C and strain rate of  $6.67 \times 10^{-4} \text{ s}^{-1}$ ).

$\epsilon$  is the true strain

$\alpha$  is the maximum strain sensitivity which corresponds to the log true strain where there is a maximum slope of the log-log plot of true stress-true strain curve (value of -0.73 at 30 °C,  $\epsilon = 0.19$  and a strain rate of  $6.67 \times 10^{-4} \text{ s}^{-1}$ ).

$\beta$  is a constant which is indicative of the extent of variation of log-log plots of true stress and true strain. The numerical value is given by,  $\beta = (A - B)(4 \times n_i)^{-1}$ . (Value of 0.11 at 30 °C,  $\epsilon = 0.19$  and a strain rate of  $6.67 \times 10^{-4} \text{ s}^{-1}$ ).

#### 5. Conclusions

The detailed analysis of flow stress and strain hardening behaviour as well as the variation of the fraction of martensite induced with strain at 30 °C for AISI 301 stainless steel has demonstrated that the strain hardening behaviour at relatively high levels of plastic strain, can be adequately described by

a sigmoidal equation. This indicates that there is a correlation between the instantaneous strain hardening behaviour and the fraction of martensite induced. The strain-induced martensitic phase transformation is therefore believed to be responsible for the sigmoidal flow stress behaviour observed in this metastable austenitic stainless steel.

The instantaneous strain hardening exponent and the extent of strain hardening both increases up to a maximum as the percentage of transformed martensite increases up to the point of martensitic saturation. The high levels of instantaneous strain hardening results in a remarkable increase in strength.

The material processing in industrial practice is not performed at 30 °C only. The variation of the instantaneous strain hardening exponent, the strength coefficient,  $K$ , and strain sensitivity,  $\alpha$  as a function of temperature will therefore be investigated in further work.

## 6. Acknowledgements

The authors are grateful to Columbus Stainless Steel company for financial support as well as the supply of materials, AMI-FMDN, administered by Mintek for supporting this work.

## 7. References

- [1] D. P. R. Palaparti, B. K. Choudhary, E. I. Samuel, V. S. Srinivasan, and M. D. Mathew, "Influence of strain rate and temperature on tensile stress – strain and work hardening behaviour of 9Cr – 1Mo ferritic steel," *Mater. Sci. Eng. A*, vol. 538, pp. 110–117, 2012.
- [2] G. E. Dieter and D. J. Bacon, *Mechanical metallurgy*, vol. 3. New York: McGraw-hill, 1986.
- [3] J. W. Simmons, "Strain hardening and plastic flow properties of nitrogen-alloyed Fe-17Cr-(8-10)Mn-5Ni austenitic stainless steels," *Acta Mater.*, vol. 45, no. 6, pp. 2467–2475, 1997.
- [4] T. W. Mukarati, R. J. Mostert, and C. W. Siyasiya, "The direct observation of surface martensite formation upon cooling to temperatures close to ambient in a heat treated AISI 301 stainless steel," *Mater. Sci. Eng. Conf. Ser.*, vol. 430, no. 1, p. 12042, 2018.
- [5] T. W. Mukarati, R. J. Mostert, and C. W. Siyasiya, "Effect of temperature and strain on martensite transformation in a high-nitrogen low-carbon AISI 301 metastable austenitic stainless steel," *Unpubl. Work*, 2019.
- [6] G. C. Soares, M. Carla, M. Rodrigues, and L. D. A. Santos, "Influence of Temperature on Mechanical Properties , Fracture Morphology and Strain Hardening Behavior of a 304 Stainless Steel," *Mater. Res.*, 2017.
- [7] J. Talonen, P. Nenonen, G. Pape, and H. Hänninen, "Effect of strain rate on the strain-induced  $\gamma \rightarrow \alpha'$ -martensite transformation and mechanical properties of austenitic stainless steels," *Metall. Mater. Trans. A*, vol. 36, no. 2, pp. 421–432, 2005.